Biophysical Journal Volume 77 September 1999 1445–1457

Polymer-Cushioned Bilayers. I. A Structural Study of Various Preparation Methods Using Neutron Reflectometry

J. Y. Wong,* J. Majewski,# M. Seitz,* C. K. Park,* J. N. Israelachvili,* and G. S. Smith#

*Department of Chemical Engineering, University of California, Santa Barbara, California 93106; and #Manuel Lujan, Jr. Neutron Scattering Center, Los Alamos National Laboratory, Los Alamos, New Mexico 87545 USA

ABSTRACT This neutron reflectometry study evaluates the structures resulting from different methods of preparing polymer-cushioned lipid bilayers. Four different techniques to deposit a dimyristoylphosphatidylcholine (DMPC) bilayer onto a polyethylenimine (PEI)-coated quartz substrate were examined: 1) vesicle adsorption onto a previously dried polymer layer; 2) vesicle adsorption onto a bare substrate, followed by polymer adsorption; and 3, 4) Langmuir-Blodgett vertical deposition of a lipid monolayer spread over a polymer-containing subphase to form a polymer-supported lipid monolayer, followed by formation of the outer lipid monolayer by either 3) horizontal deposition of the lipid monolayer or 4) vesicle adsorption. We show that the initial conditions of the polymer layer are a critical factor for the successful formation of our desired structure, i.e., a continuous bilayer atop a hydrated PEI layer. Our desired structure was found for all methods investigated except the horizontal deposition. The interaction forces between these polymer-supported bilayers are investigated in a separate paper (Wong, J. Y., C. K. Park, M. Seitz, and J. Israelachvili. 1999. *Biophys. J.* 77:1458-1468), which indicate that the presence of the polymer cushion significantly alters the interaction potential. These polymer-supported bilayers could serve as model systems for the study of transmembrane proteins under conditions more closely mimicking real cellular membrane environments.

INTRODUCTION

Solid-supported membranes are being used increasingly as well-defined model systems for fundamental biophysical research and have been proposed as surfaces for the immobilization of proteins integral to biosensors (Sackmann, 1996). One major obstacle, however, has been the successful incorporation of *transmembrane* proteins into solid-supported membranes. To date, there are only a few examples of transmembrane proteins that retain their activity after incorporation into such bilayers (McConnell et al., 1986; Salafsky et al., 1996; Hinterdorfer et al. 1994). Furthermore, even when the activity is retained, a large fraction of incorporated protein may become immobilized (Kalb and Tamm, 1992a) since the distance the protein protrudes from the membrane is often much larger than the aqueous space formed between the substrate and the biomembrane (typically 10–20 Å).

It is desirable to create model systems that maintain the structural and dynamic integrity of free biomembranes, for example, supports that do not hinder the lateral mobilities of membrane components. This is important because a wide variety of biological processes involve the recruitment, multimerization, transport, and assembly of specific membrane proteins and lipids. One promising strategy for decoupling the biomembrane from the underlying surface is to rest the biomembrane on a soft cushion composed of a water-swellable hydrophilic polymer or polyelectrolyte film (Kühner and Sackmann, 1996; Sackmann, 1996; Majewski et al., 1998). The polymer layer acts as a support for the biomembrane, not unlike the cytoskeletal support found in actual mammalian cell membranes (Jacobson et al., 1995).

Several strategies can be used for the assembly of biomembranes onto various solid supports and have been recently reviewed (Sackmann, 1996; Steinem et al., 1996; Puu and Gustafson, 1997). The two major techniques are direct vesicle fusion (Horn, 1984; Bayerl and Bloom, 1990) and the Langmuir-Blodgett (LB) technique (Tamm and McConnell, 1986). Furthermore, these two techniques can be combined, i.e., adsorption of vesicles onto pre-formed monolayers as described by various authors (Spinke et al., 1992; Kalb et al., 1992b). While solid-supported membranes have been studied extensively, it is not clear how the presence of a polymer layer would affect the assembly process of the biomembrane.

In this paper, we investigated the structures resulting from four different methods of preparing polyethylenimine (PEI)-supported dimyristoylphosphatidylcholine (DMPC) bilayers (Fig. 1) with neutron reflectivity. This well-established technique has already been used to probe the structure of solid-supported bilayers (Johnson et al., 1991; Koenig et al., 1996). Neutron reflectivity data can be regressed to give the films' density profile. It is then possible to infer the bilayer surface coverage, individual layer thicknesses, hydration of the polymer layer, and the relative positions of each layer in the direction normal to the substrate. This enables us to gain a structural picture of the molecular assemblies formed from the various preparation techniques.

Received for publication 9 February 1999 and in final form 7 June 1999.

Address reprint requests to Dr. Gregory S. Smith, Manuel Lujan, Jr. Neutron Scattering Center, H805, Los Alamos National Laboratory, Los Alamos, NM 87545. Tel.: 505-665-2842; Fax: 505-665-2676; E-mail: gsmith@lanl.gov.

J. Y. Wong's current address is Department of Biomedical Engineering, Boston University, 44 Cummington Street, Boston, MA 02215.

0006-3495/99/09/1445/13 $2.00

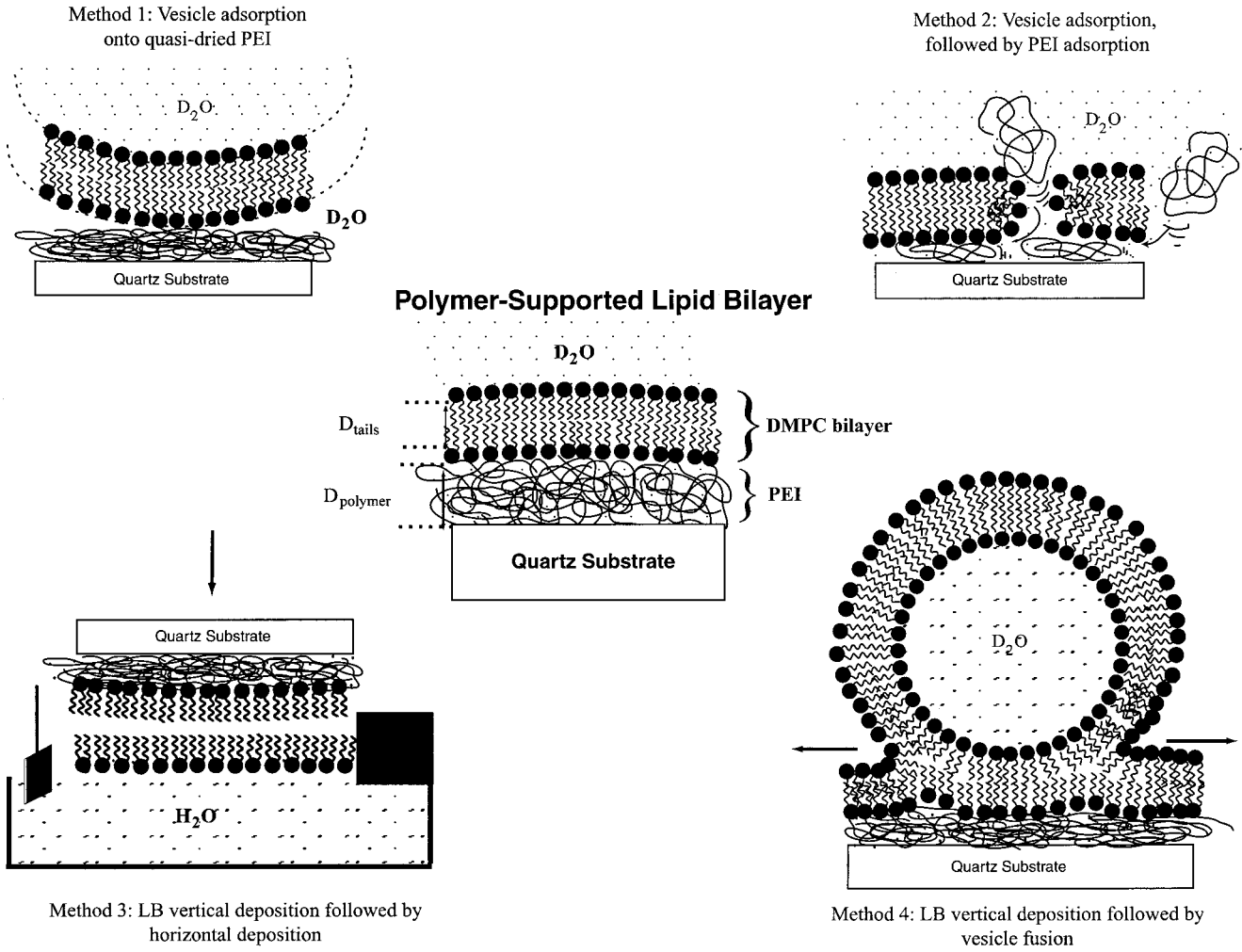

FIGURE 1 Schematic of the procedures used to prepare polymer-cushioned bilayers that were then investigated with neutron reflectivity. The methods are labeled as described in the Materials, Results, and Discussion sections. Our desired structure is in the center of the diagram.

Experimental

Materials

Branched PEI (M_w = 1800 g/mol, 95% purity) was obtained from Polysciences (Warrington, PA). DMPC (M_w = 678 g/mol, >99% purity) was purchased from Avanti Polar Lipids (Alabaster, AL). D_2O (99.9%) was obtained from Sigma (St. Louis, MO), and potassium nitrate was purchased from Alfa (Puratronic grade, Ward Hill, MA).

Small unilamellar vesicles (SUVs) of DMPC were prepared following the method of Bangham et al. (1974). Briefly, multilamellar vesicles (MLVs) were prepared by hydrating a dried lipid film of DMPC in Millipore water (37°C for several hours), subsequently sonicating with a probe sonicator (Fisher Sonic Dismembrator 300) and filtering through a 0.22 μm Millipore filter. The resulting SUVs have an average diameter of 400 Å as found by particle sizing optical turbidity measurements (Microtrac UPA 150, Brookhaven Instruments Corp.). The vesicle suspension was added from an aqueous stock solution of 1 mg/ml.

The monocrystalline quartz substrates used for neutron reflectometry were purchased from Atomergic Chemetals Corp. (Farmingdale, NY) and were polished to a flatness better than $\lambda/10$ and scratch/dig, S/D = 80/60. The quartz substrates were cleaned in aqua regia, rinsed in Milli-Q water, and cleaned for at least 30 min in a Jelight Model # 342 UV ozone cleaner.

Preparation methods for polymer-supported bilayers

The liquid-solid interface cell (flow cell) used for the measurements is shown schematically in Fig. 2 (Baker et al., 1994). All solutions were allowed to adsorb for at least 15 min before data collection. All preparations and measurements were done above the chain melting temperature of DMPC, 24°C.

We investigated four different procedures for preparing polymer-supported bilayers (Fig. 1) onto quartz substrates: 1) formation of polymer (PEI) layer (adsorbed, rinsed, and dried in air), followed by addition of vesicles to the PEI layer in the flow cell; 2) vesicle fusion on a bare quartz substrate in the flow cell, followed by addition of PEI; 3) LB deposition of a PEI-supported DMPC monolayer (PEI present in the subphase), followed by horizontal deposition of the outer DMPC layer; and 4) LB deposition of the PEI-supported DMPC monolayer, followed by vesicle fusion. Specific details of each method are given below.

Method 1: vesicle fusion on dried polymer

The quartz substrate was immersed in a 100 ppm PEI solution of 0.5 mM KNO_3/H_2O (Milli-Q water, pH ~7, 15 min) and allowed to dry for several hours (typically, 4 h). Shorter or longer drying times would not likely be a

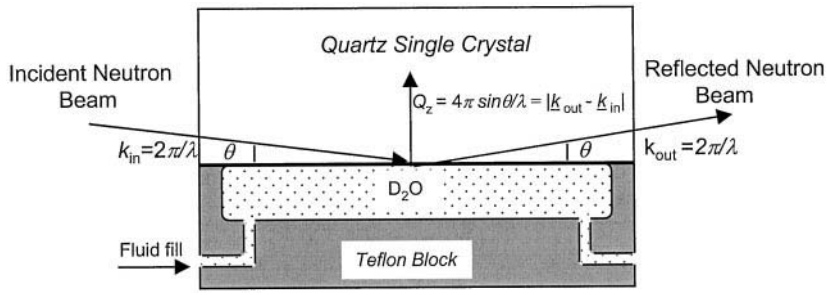

FIGURE 2 Diagram of the liquid-solid interface cell used for neutron reflectivity measurements. The neutron beam probes the solid-solution interface. The only surfaces of the system in contact with the aqueous solution are the quartz substrate and the Teflon portion of the fluid cell.

crucial factor. The neutron reflectivity curve was then measured against air. In the second step, the PEI-coated quartz was transferred into the flow cell which was filled with D_2O, and DMPC vesicles were added from an aqueous stock suspension (1 mg/ml) to a final concentration of 0.14 mg/ml DMPC. The neutron reflectivity spectrum was then measured.

Method 2: polymer adsorption on bilayers (reverse method)

The flow cell was fitted with a quartz substrate and then filled with a solution of 150 mM KNO_3/D_2O, followed by addition of DMPC vesicles (final concentration, 0.14 mg/ml). After the reflectivity curve of the DMPC vesicles on the bare quartz substrate was measured, PEI was added to the system as a 100 ppm solution in 150 mM KNO_3/D_2O. The reflectivity curve was then remeasured.

Method 3: Langmuir-Blodgett vertical deposition followed by a Langmuir-Schaefer horizontal deposition of DMPC monolayers (LB-LS)

A monolayer of hydrogenated DMPC spread at the air-liquid interface of a PEI-containing subphase (100 ppm PEI in 0.5 mM KNO_3/H_2O) was deposited onto the quartz block using the LB method ($\Pi = 30 \pm 2$ mN/m; Joyce-Loebl Langmuir Trough IV). Subsequently, we used the horizontal deposition method to pass the quartz substrate (coated with a PEI-DMPC monolayer) through a monolayer spread onto a pure Millipore water subphase. The liquid-solid interface cell was then assembled under water. The Millipore water was later exchanged by carefully flushing with a 0.5 mM KNO_3/D_2O solution. The reflectivity curve was then measured.

Method 4: vesicle fusion on polymer supported monolayer ("LB-vesicle fusion")

Again, a monolayer of hydrogenated DMPC spread at the air-liquid interface of a PEI-containing subphase (100 ppm PEI in 0.5 mM KNO_3/H_2O) was deposited onto the quartz substrate using the LB method as described in the LB-LS method. The DMPC-PEI layer was prepared ~15 min before measurement of the neutron reflectivity in air. In a second step (after 4 h), the substrate was assembled into the flow cell and a vesicle solution (final concentration 0.14 mg/ml DMPC) in 0.5 mM KNO_3/D_2O was added. The reflectivity curve was then measured.

Neutron reflectivity measurements in the liquid-solid interface cell (flow cell)

The neutron reflectivity measurements were performed on the Surface Profile Analysis Reflectometer (SPEAR, Manuel Lujan, Jr. Neutron Scattering Center, Los Alamos National Laboratory). SPEAR is a time-of-flight reflectometer employing a polychromatic, pulsed neutron source. The basic principle of neutron reflectometry involves directing a collimated neutron beam onto a flat interface at a low incidence angle, θ, and measuring the ratio of reflected to incident intensity, R, as a function of momentum transfer $Q_z = 4\pi \sin\theta/\lambda$, where λ is the neutron wavelength. The range of neutron wavelengths used in the experiments presented here was 1–16 Å, determined using the time-of-flight technique.

We used two different geometries to probe the surface of the quartz substrate. When we probed the surface against air, the experiments were performed in an "upright" geometry, i.e., the quartz on the bottom against air above. When we probed the solid-liquid interface, we used an "inverted" geometry (Fig. 2), i.e., D_2O on the bottom against quartz above. In both cases the lower medium had a higher scattering length density than the upper one. Under these conditions, the reflectivity $R = 1$ for Q_z below a critical value $Q_c = 4(\pi\Delta\beta)^{1/2}$, where $\Delta\beta$ is the scattering length density difference between the lower and upper media. Above Q_c, R decays with Q_z (the details depend on the area-averaged scattering length density profile normal to the interface). In order to achieve an adequate range of Q_z, typically two different θ were used for each run; data from low- and high-angle runs had a substantial range of Q_z in common, which was matched to obtain the complete R vs. Q_z profile. Neutron reflectivity data collection typically lasted 3–4.5 h.

The reflectivity data were reduced using the incident neutron intensity spectrum and plotted as $R^* Q_z^4$ versus the perpendicular scattering vector, Q_z (this accounts for the sharp Q_z^{-4} decrease of the reflectivity due to Fresnel's law). The error bars on the data represent the statistical errors in the measurements where the uncertainty in the Q_z resolution, $(\sigma_{Qz})/Q_z$, was nearly constant over the measured scattering vector range with a value of ~3%.

All scattering length densities presented in this paper are absolute scattering length densities, i.e., given with air as a reference. The various layers (phospholipid membrane, PEI polymer, etc.) were modeled as boxes of a specified thickness and scattering length density. The data were fit considering one box to describe the lipid bilayer,[1] and the reflectivities were calculated using the iterative, dynamical method (Russell, 1990). One overall root-mean-square roughness factor, σ, was used to smear out all of the interfaces (Als-Nielsen, 1986; Nevot and Croce, 1980). The fits included an additional parameter to normalize the calculated reflectivity to the data. Based on this input, a "model" reflectivity profile was generated and compared to the actually measured reflectivity profile. The model was then adjusted to obtain the best least-squares fit to the data (see Appendix).

RESULTS

The neutron reflectivity profile of the pure quartz substrate measured in contact with D_2O gave a roughness parameter

[1]Since the contrast between hydrogenated tails and D_2O is the highest, the box represents mostly the lipid tails. However, the length of the box averages over both the tails and the DMPC headgroups. Since the scattering contrast between hydrated headgroups and D_2O is not vanishing, this averaging results in the lengths that are larger than the lengths of the tails but smaller than the total length of the lipid bilayer, as seen by x-ray scattering by Janiak et al.

(σ) of 5.0 ± 1.0 Å; $\chi^2 = 5.3$. The scattering length density, β, of quartz was 4.2×10^{-6} Å^{-2} (air as reference medium). This value for β_{quartz} was used for all of the fitting procedures described below for the four different preparation methods.

Method 1: vesicle fusion on dried polymer

In previous studies, we used neutron reflectivity to probe the structure formed at the quartz-solution interface after adsorbing DMPC vesicles to a swollen PEI-coated quartz substrate and found a very complicated neutron reflectivity profile (Fig. 3). From our analysis, we concluded that the structure was comprised of bilayer aggregates and/or unfused vesicles with a characteristic length scale of ~600 Å. However, we found that if there was *no polymer* present, i.e., addition of DMPC vesicles onto a *bare* quartz substrate, this scenario led to an almost perfect bilayer, as previously observed (Johnson et al., 1991). Clearly, the presence of the PEI layer strongly influences the DMPC vesicles' adsorption behavior and fusion into other structures.

In our previous studies that led to the complex aggregate structure, the final assembly had been formed by injecting a vesicle solution directly into the flow cell to allow adsorption at the wet PEI-quartz interface. Here, we allowed the polymer layer to dry in air *before* exposure to the vesicle solution. The neutron reflectivity curve of the *dried* PEI layer on quartz *against air* is shown in Fig. 4 *a*. The scattering profile of the polymer layer could not be fit with simple one- or two-box models. Satisfactory fits were achieved only with a profile described by a negative step-like scattering length density profile that indicates the presence of H_2O (decreasing in concentration in the direction normal to the surface) within the PEI layer (Fig. 4 *a, inset*; Table 1, Method 1, step (a); Appendix). Using the parameters from the fitting procedure (Table 1; Appendix, Eq. 1), we found that the PEI layer is significantly hydrated with an *average* volume ratio of PEI/H_2O ~1:3. Thus, the PEI layer retains a large amount of water and is in a *quasi-dried* state.

After the addition of a DMPC vesicle-D_2O solution to the quasi-dried PEI layer, the resulting reflectivity curve (Fig. 4 *b*) can be fit almost perfectly with the parameters shown in Table 1 (Method 1, step (b)) and Fig. 4 *b, inset* (note that H_2O concentration is decreasing). The results clearly show the presence of a lipid bilayer on top of a polymer layer, which is, in turn, supported by the quartz substrate. From the fitting procedure we found that the total thickness of the PEI layer increases from ~110 Å in the quasi-dried state to

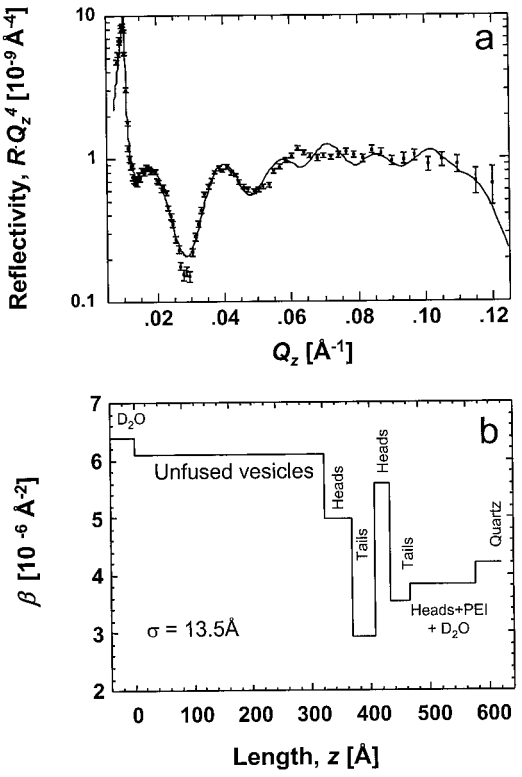

FIGURE 3 (*a*) Neutron reflectivity curve after DMPC vesicle adsorption on wet PEI in D_2O solution. The solid curve through the data is the result of a multiple box fit. (*b*) Corresponding scattering length density profile of the multiple box model (adapted from Majewski et al., 1998). The model presented here is not unique, but shows that the length scales are ~600 Å.

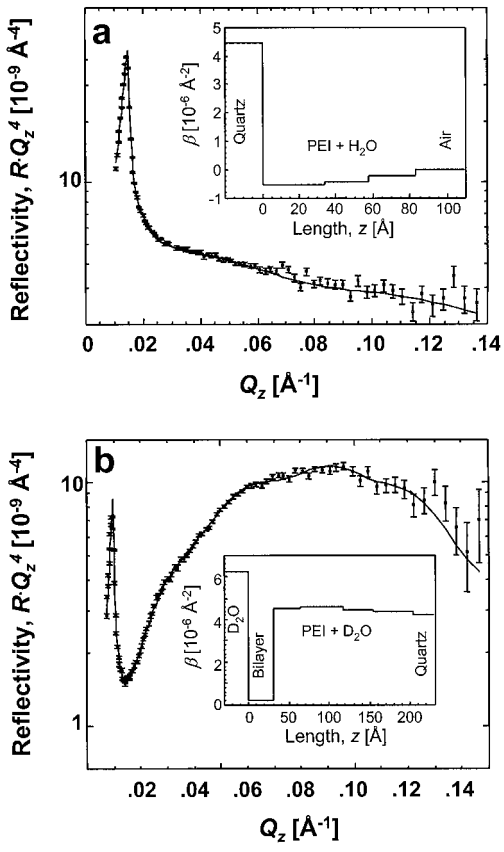

FIGURE 4 (*a*) Neutron reflectivity data of a dried PEI-H_2O layer against air. After exposure to the PEI-H_2O solution for 4 h, the quartz substrate was rinsed with water and dried in air for 4 h. (*b*) Neutron reflectivity data of the dried polymer layer after exposure to the DMPC vesicle solution in the flow cell (vesicle fusion on dry polymer method); measurement against D_2O. Insets show the fitted scattering length density profiles (Table 1).

TABLE 1 Comparison of neutron reflectivity data for methods 1–4

	σ (Å)	β lipid tails (10^{-6} Å^{-2})	D lipid tails (Å)	β polymer (10^{-6} Å^{-2})	D polymer (Å)	χ^2
Method 1: Vesicle fusion on dry polymer (Fig. 4)						
Step (a)	4.9 (7)	—	—	−0.30 (6)#	107.7 (3.0)*	22.6
Step (b)	5.6 (5)	0.16 (10)	31.3 (8)	4.48 (4)#	172.9 (3.8)*	14.2
Method 2: Polymer adsorption on bilayers (reverse method, Fig. 5)						
Low Salt* (0.5 mM KNO_3, Majewski et al., 1998)						
Step (a)	5.8 (4)	0.77 (8)	31.9 (6)	—	—	1.9
Step (b)	6.7 (4)	0.77 (8)	31.9 (6)	5.19 (3)	40.4 (9)	3.0
High Salt (150 mM KNO_3)						
Step (a)	2.2 (4)	−0.1 (6)	36.1 (4)	—	—	3.8
Step (b)	2.3 (1)	0.38 (6)	36.1 (4)	5.40 (2)	48.3 (0.6)	3.4
Method 3: Langmuir-Blodgett vertical and horizontal deposition (LB-LS, Fig. 6)						
	7.3 (0.6)	0.7 (2)	11.4 (0.7)	4.32 (1)	72.2 (2.2)	7.6
Method 4: Vesicle fusion on monolayer ("LB-vesicle fusion," Fig. 7)						
Step (a)	3.0 (1)	−0.41 (4)	23.6 (2.4)	0.02 (1)	43.2 (2.3)	15.9
Step (b)	6.0 (3)	0.39 (9)	33.7 (6)	4.48# (2)	144* (2)	5.4

D refers to the thickness of the specified box, and β to the scattering length density (air as reference medium); σ is the Gaussian roughness of the interface. We used the reduced χ^2; for an excellent fit, the χ^2 should be ~1.
*D of the polymer is the total thickness obtained from the separate boxes.
#β of the polymer is the averaged value of the boxes.

~180 Å in the hydrated state, i.e., an increase in thickness by a factor of ~1.6. From our data, the corresponding change in the volume ratio, PEI/water, can be estimated. This gives ~15–20 vol % polymer in the hydrated layer (see Appendix).

From the fit, the thickness of the tails of the DMPC bilayer is ~30 Å (Table 1, Method 1). Also, by employing Eq. 1 and the determined $\beta_{\text{lipidtails}}$ (Table 1, Method 1), the calculated surface coverage of the DMPC bilayer on the PEI-coated quartz surface is 94% (see Appendix). We therefore find the structure obtained from vesicle adsorption onto a quasi-dried polyelectrolyte layer to be a fairly complete DMPC bilayer atop a highly hydrated PEI layer.

Method 2: polymer adsorption on bilayers (reverse method)

As described above, our earlier neutron reflectivity studies showed that DMPC vesicles adsorb to a bare quartz substrate, forming an almost perfect bilayer directly on the quartz substrate (Majewski et al., 1998). Subsequent addition of the polymer solution led to our desired structure in which the polymer lies *underneath* the bilayer. From those results (low salt conditions, 0.5 mM KNO_3), we concluded that the polymer must be able to crawl underneath the formed bilayer, probably via defects in its structure. Here, we present the results obtained from repeating these earlier experiments but under more physiological conditions, i.e., 150 mM KNO_3. This monovalent salt was chosen over NaCl for easier comparison with recent SFA results (Wong et al., submitted for publication).

Fig. 5 *a* shows the scattering profile of the DMPC bilayer formed directly on the quartz substrate under these high salt conditions. As we saw previously for the low salt condition (Majewski et al., 1998), the fit using the simple one-box model (Fig. 5 *b*) is quite good and gives a value of 36 Å for the lipid tails (Table 1). During the fitting process, the use of a more complicated three-box model to account for the lipid headgroups did not significantly increase the quality of the fit or the value of χ^2 (data not shown). The scattering length densities of the bilayer composed of the hydrogenated lipid tails under the high and low salt conditions (Table 1, Method 2, step (a)) can be used to determine the differences in surface coverage for the two cases. From these fitted densities we find that the lipid membrane in the high salt concentration occupies almost 98% of the surface (an almost perfect bilayer) compared to 85% in the low salt case.

After adding PEI to the system, we observed a significant change in the neutron reflectivity curve (Fig. 5 *a*). Our fit shows that the observed change can be attributed to a swollen polymer (PEI/D_2O) layer between DMPC bilayer and the quartz substrate (Fig. 5 *c*). There is no change in the thickness of the lipid tails and only a moderate increase in their scattering length density. When we compare these results to our earlier studies (Majewski et al., 1998), we find that the volume fraction of D_2O in the PEI layer in high salt (83%) agrees with that measured for the low salt conditions (79%). In the high salt case, the overall roughness increased only slightly as compared with the DMPC bilayer on bare quartz, but we observed a change in the scattering length density of the lipid tails (Table 1, Method 2, step (b)). This indicates that the high packing density of the hydrocarbon chains of the bilayer (98%) was partly reduced (91%) by the addition of the PEI resulting in a significant amount of penetration of D_2O or PEI-D_2O into the bilayer region. Such a perturbation of the DMPC bilayer by the PEI layer was not observed in the low salt case.

In order to test the structural stability of the polymer-supported bilayer under high salt conditions, we rinsed the

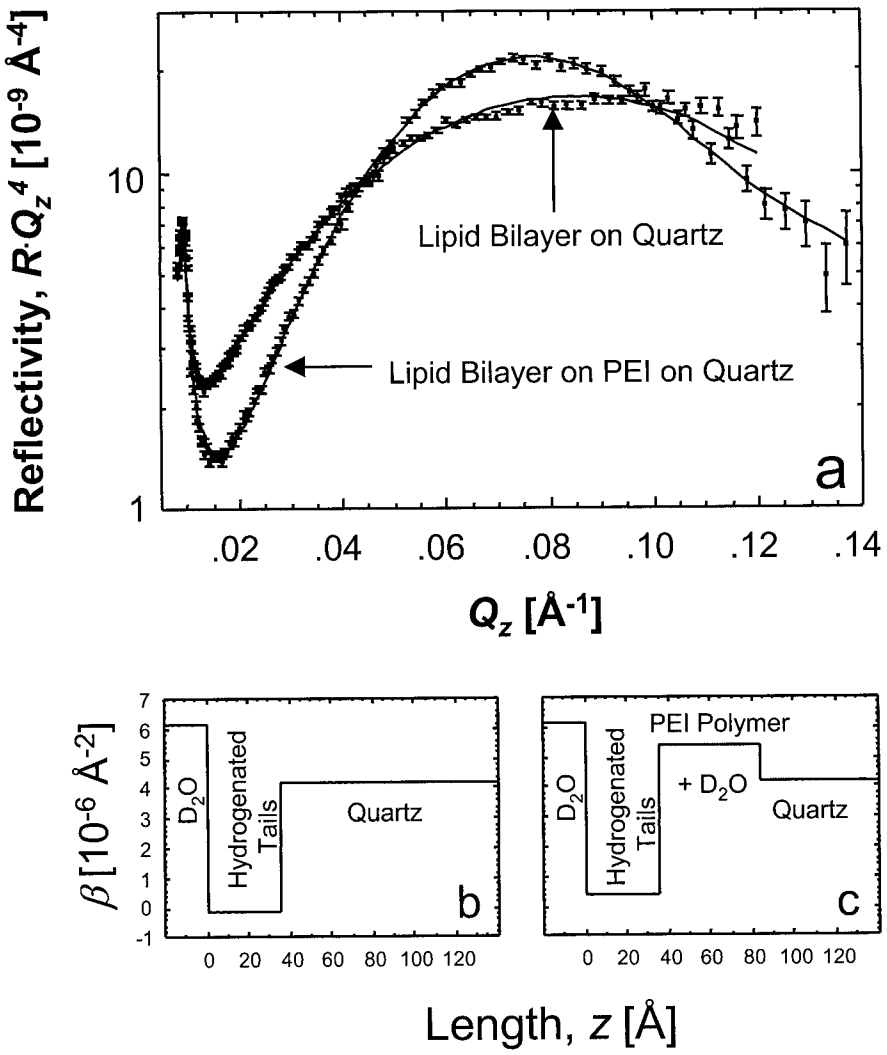

FIGURE 5 Neutron reflectivity data of a DMPC bilayer on a bare quartz substrate, followed by PEI adsorption (polymer adsorption on bilayer (reverse)) (high salt, 150 mM KNO_3). The bottom part of the figure shows the corresponding scattering length density profiles.

system with 150 mM salt solution and measured only the low Q_z portion of the neutron reflectivity curve (0.008 Å^{-1}-0.075 Å^{-1}, data not shown). Although the fitting procedure of the data with the smaller Q_z range gives bigger uncertainties in the fitting parameters, we found that the rinsing had no effect on the membrane. These results confirm our earlier studies and further show that the reverse preparation procedure gives our desired structure under both low salt (0.5 mM KNO_3) and high salt (150 mM KNO_3) conditions.

Method 3: LB vertical deposition followed by an LS horizontal deposition of DMPC monolayers (LB-LS)

We used the LB vertical dipping method to deposit a PEI-supported monolayer of hydrogenated DMPC onto a quartz substrate. After the formation of the first monolayer, which was later confirmed by neutron scattering (Method 4, vesicle fusion on monolayer method; cf. Fig. 7 *a* and Table 1, Method 4, step (a)), we attempted to add a second DMPC monolayer using the LS horizontal dipping method. Fig. 6 shows the scattering profile of the resulting structure. From the fit, the value for the thickness of the DMPC lipid tails is ~11 Å (Table 1, Method 3). Thus, the horizontal dipping method did not give our desired polymer-supported bilayer structure.

Method 4: vesicle fusion on polymer supported monolayer ("LB-vesicle fusion")

Again, we used the LB vertical dipping method to deposit a PEI-supported monolayer of hydrogenated DMPC onto a quartz substrate. Before adding the vesicle solution, we first characterized the PEI-supported DMPC monolayer by measuring the neutron reflectivity spectrum in air (Fig. 7 *a*; Table 1, Method 4, step (a)). The structure could be fit with a two-box model: one box ~24 Å thick for the DMPC monolayer and one 43-Å-thick box for the PEI-H_2O layer (Fig. 7 *a, inset*; Table 1, Method 4).

After exposure to a vesicle solution, the resulting reflectivity curve (Fig. 7 *b*) indicates that an ~34 Å (Table 1,

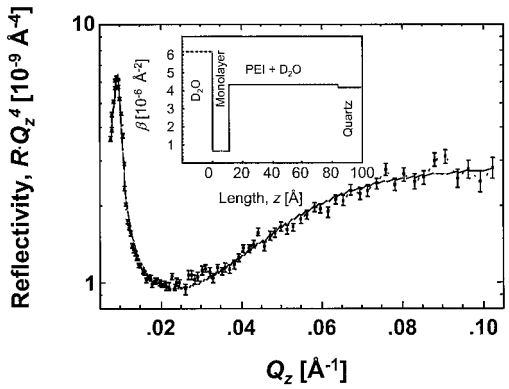

FIGURE 6 Neutron reflectivity curves obtained after applying the horizontal dipping procedure (LB-LS method) to prepare polymer-cushioned bilayers. Inset shows the fitted scattering length density profile β. The obtained thickness, 11 Å, suggests the presence of a single monolayer of hydrogenated DMPC.

Method 4) bilayer was formed on the polymer support. We found that the simplest model that could satisfactorily fit the reflectivity curve had four boxes: one box for the lipid tails and three in series to approximate the scattering length density profile of the aqueous (or hydrated) PEI-layer (Table 1, Method 4, step (b); Fig. 7 *b, inset*). We found the calculated surface coverage of the bilayer to be ~90%. Moreover, the PEI layer appears to undergo swelling, increasing its thickness threefold from its quasi-dry state (50% PEI, $D_{polymer} \sim 45$ Å) to its final hydrated state (~15–20% PEI, $D_{polymer} \sim 145$ Å, see Appendix) upon exposure to the vesicle solution. In short, vesicle adsorption on polymer-supported lipid monolayers also allows the formation of fairly complete DMPC bilayers atop a highly hydrated polymer layer.

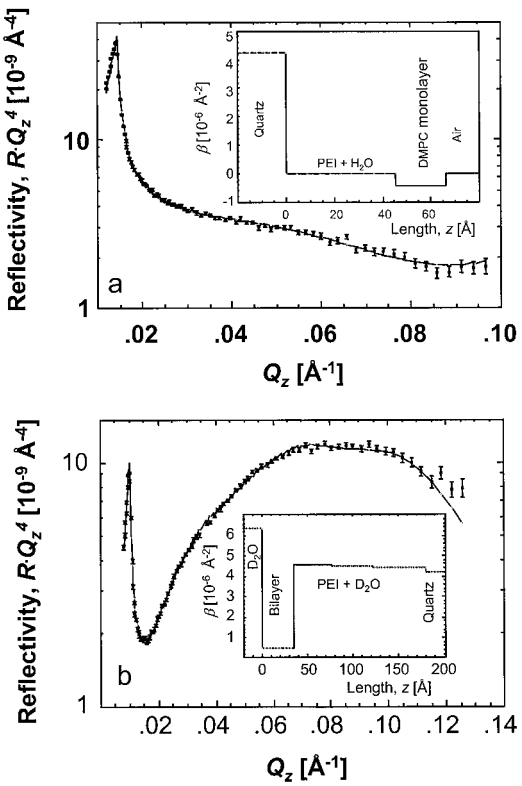

FIGURE 7 Neutron reflectivity data illustrating vesicle fusion on monolayer method to prepare a polymer-cushioned bilayer. (*a*) After LB deposition of PEI-DMPC monolayer; measurement in air, followed by (*b*) vesicle fusion onto the quartz block coated with PEI-DMPC monolayer transferred into the flow cell; measurement against D_2O. Insets show the corresponding scattering length density profiles.

DISCUSSION

As a continuation of our previous neutron reflectivity studies (Majewski et al., 1998), we further investigated the adsorption of small unilamellar lipid vesicles directly onto a polymer-covered quartz substrate to prepare softly supported biomembranes. As the results from the vesicle fusion on dry polymer method indicate, the initial drying of the PEI layer before the addition of DMPC vesicles appears to be a critical step needed to form a polymer-cushioned bilayer. This important finding, discussed further below, is in stark contrast to our previous studies when we *did not* allow the polymer to dry, which resulted in a complex structure consisting mainly of bilayer aggregates and/or unfused vesicles. Moreover, the successful realization of polymer-cushioned lipid bilayers by this simple procedure promises the straightforward incorporation of transmembrane proteins into softly supported lipid bilayers.

In addition, we confirmed that a reverse procedure in which bilayers are formed on a quartz substrate first and subsequently treated with PEI solution ("polymer added to bilayer" method) can also be used to form polymer-supported lipid bilayers, under both low (0.5 mM) and high (150 mM KNO_3) salt conditions. Specifically, this technique resulted in 94% complete bilayers (32 Å) on a 40-Å-thick 3:1 water/PEI layer (Table 1). For the high salt case, 98% bilayers (36 Å) were obtained on a 48-Å-thick water/PEI layer.

The success of this method shows the importance of balancing the interaction forces between the various components of these assemblies. In our case, there appears to be a strong interaction between the positively charged PEI layer and the negatively charged quartz substrate. This electrostatically driven attraction serves to displace the lipids with polymer. Presumably, this displacement is aided through defects and flaws in the bilayer.

The situation where the bilayer-substrate attraction dominates the polymer-substrate interaction has been reported. The research group of Sackmann observed that for lipid membranes on dextran, the polymer had to be covalently attached to the underlying substrate in order to prevent the collapse of the lipid-polymer composite film (Elender and Sackmann, 1994; Kühner and Sackmann, 1996).

It is worth noting that the polymer adsorption on bilayers (reverse method) is an extremely simple method to create polymer-supported biomembranes, in addition to being of

theoretical interest. It is also apparent that variations in the molecular structure of the components can affect the stability of a polymer-supported membrane system in a subtle way. Therefore, the polymer adsorption on bilayer method cannot be generalized a priori as being useful for other substrate-polymer-lipid systems. Besides, it seems to be only of limited practical use for the preparation of more biologically relevant architectures, e.g., bilayer with incorporated proteins, since the first step involves the fusion of vesicles onto the bare quartz substrate. When the simple lipid vesicles used in our studies are replaced by proteoliposomes, the presence of transmembrane proteins may prevent the subsequent formation of the underlying polymer cushion.

Although in the two methods discussed so far the resulting bilayer structure is determined entirely by the composition of the adsorbed lipid vesicles, a stepwise approach allows the construction of more complex membrane architectures. Namely, in the LB-LS and vesicle fusion on monolayer methods we investigated the deposition of a first (proximal) lipid monolayer onto the polymer substrate followed by the separate formation of the second (distal) lipid layer by LS deposition (LB-LS) or vesicle adsorption (vesicle fusion on monolayer). Although for better comparability with the earlier preparation methods the simple DMPC bilayer system was again studied here, it should be mentioned that this approach can now easily be extended to more complex systems, in which the two lipid membrane layers can differ from each other in their composition. On the one hand, this method allows monolayer-polymer covalent attachment as well as asymmetric membranes. On the other hand, this may make transmembrane protein incorporation more difficult.

As a stepwise approach, the horizontal deposition method has been used successfully to deposit a second lipid monolayer onto robust monolayers such as, e.g., lipids and lipid mixtures (Evert et al., 1994) or thiols on gold (Steinem et al., 1996) or silanes on silicon or glass (Paddeu et al., 1995), and PEG-lipids on octadecyltrichlorosilane (OTS)-coated substrates (Kuhl et al., 1998). This method has also been described in the literature to deposit DMPC bilayers on polyacrylamide substrates (Kühner et al., 1994).

However, we found that the LB-LS method did not give us our desired PEI-cushioned DMPC bilayer structure. In fact, the low thickness of the lipid layer obtained suggests the presence of a single molecular layer on our PEI support (surface occupancy ~86%). Since a hydrophobic lipid monolayer will not be stable on the polymer cushion under water, it is reasonable to assume that a reorganization of molecules within the surface layer, as well as some depletion of lipid from the support, occurred. The resulting molecular structure most likely consists of highly tilted lipid chains of which some have "flipped" in order to provide a hydrophilic interface toward the solution, while the others remain in their original orientation with their lipid headgroups contacting the polymeric substrate. Although this remains speculative, it can be concluded that the horizontal dipping method is the least favorable for the preparation of polymer-supported lipid membranes.

In this context, it should be mentioned that technical difficulties naturally arise when one attempts to slowly push a heavy quartz block (as was required for our neutron scattering studies) in a perfectly horizontal orientation through a lipid monolayer at the air-water interface. Apart from this problem, which is related to our particular experimental setup, it is also clear that both the quality and the stability of the first monolayer are important parameters that determine the successful horizontal deposition of the second lipid layer. Our observations here are further supported by our previous experiments on mica substrates coated with polymer-supported DMPC monolayers (unpublished data), in which the formation of the outer monolayer by vertical LB deposition at a constant surface pressure failed; instead, we observed an *increase* in area during deposition suggesting that the *inner* DMPC monolayer proximal to the PEI cushion was being peeled off the substrate. This instability of the PEI-supported zwitterionic lipid monolayer in water was also confirmed from fluorescence microscopy experiments and contact angle measurements. Furthermore, these same studies showed that when the PEI-supported DMPC monolayer was directly exposed to a vesicle suspension, instead of pure water, the fluorescently labeled proximal monolayer remained on the polymeric substrate, also in agreement with the neutron results presented in this paper (Seitz et al., 1999). Thus, the interaction between DMPC and PEI is weak, and one explanation for the failure of the LB-LS method and success of the vesicle fusion on monolayer method could be a kinetic argument in which the desorption of lipid from the polymer is *faster* than lipid adsorption. This may be due to the dramatic difference in the exposure to the *number* of lipid molecules when plunging through the surface of a lipid monolayer compared to direct exposure to a vesicle solution.

An additional driving force for successful bilayer formation could be the flatness of the quasi-dry polyelectrolyte layer. In particular, the vesicle fusion on monolayer method makes use of this observation, and was found to be another useful procedure for the preparation of polymer-supported biomembranes (recall that in our previous studies, the polymer layer was not allowed to dry and led to a complex aggregate structure). While this procedure is more elaborate than the easier vesicle adsorption process on dried polymer substrates, the stepwise approach of the vesicle fusion on monolayer method will be of importance, for instance, when a partial covalent attachment of the final membrane system to the polymeric substrate is considered (Seitz et al., 1998).

It is interesting to compare our results obtained for vesicle fusion on dry polymer and monolayer methods with respect to the nature of the PEI layer before addition of the vesicle solution. It was found that in order to achieve successful bilayer formation, the polymer layer (or the polymer-supported monolayer, respectively) had to be kept initially quasi-dry. In contrast, for both methods, complex surface structures consisting of bilayer aggregates and un-

fused vesicles were observed when the polymer-coated substrates were first exposed to salt solution *before* the addition of DMPC vesicles. This suggests that a soft and fluctuating polymer substrate—although a desired final property of polymer-supported bilayer systems—is *unfavorable during the initial stages* of the preparation. As depicted in Fig. 8, a water-swollen PEI layer no longer provides a "sharp" interface on which the vesicles can spread out to form a bilayer. Instead, from our findings it seems likely that some vesicles get trapped in the "diluted" or "brush-like" polymer on the quartz substrate, which eventually leads to polymer-lipid aggregates in the interfacial layer (Fig. 8 *A*). However, when a quasi-dried substrate is directly treated with a vesicle solution, the formation of a lipid bilayer appears to proceed fast enough to prevent the trapping of vesicles or rehydration of the polymer cushion (Fig. 8 *B*).

In order to establish an understanding of the described observations for the vesicle fusion on monolayer method on a molecular level, it is important to refer to kinetic studies of the vesicle adsorption process on solid-supported lipid monolayers recently presented by Lingler et al. (1997). In their studies employing surface plasmon and impedance spectroscopy, DMPC vesicles were found to form a bilayer structure on thiolipid films on gold in a process consisting of three kinetic regimes. In a first, diffusion-controlled step, the thickness of the surface layer increased quickly within the first 20 s after vesicle injection. This could be related to an adsorption of the vesicles to the hydrophobic monolayer surface, possibly involving their rupture during the early stages of the bilayer formation. It was further suggested that in a second intermediate time regime ($t = 5$ min) the lateral spreading of the outer monolayers from adsorbed vesicles proceeded almost to completion. Finally, in a third kinetic regime, the adsorption of lipid molecules to an almost fully occupied surface bilayer membrane was completed within the next 3 h.

To guarantee successful bilayer formation during vesicle adsorption on PEI, it is important to prevent the depletion of

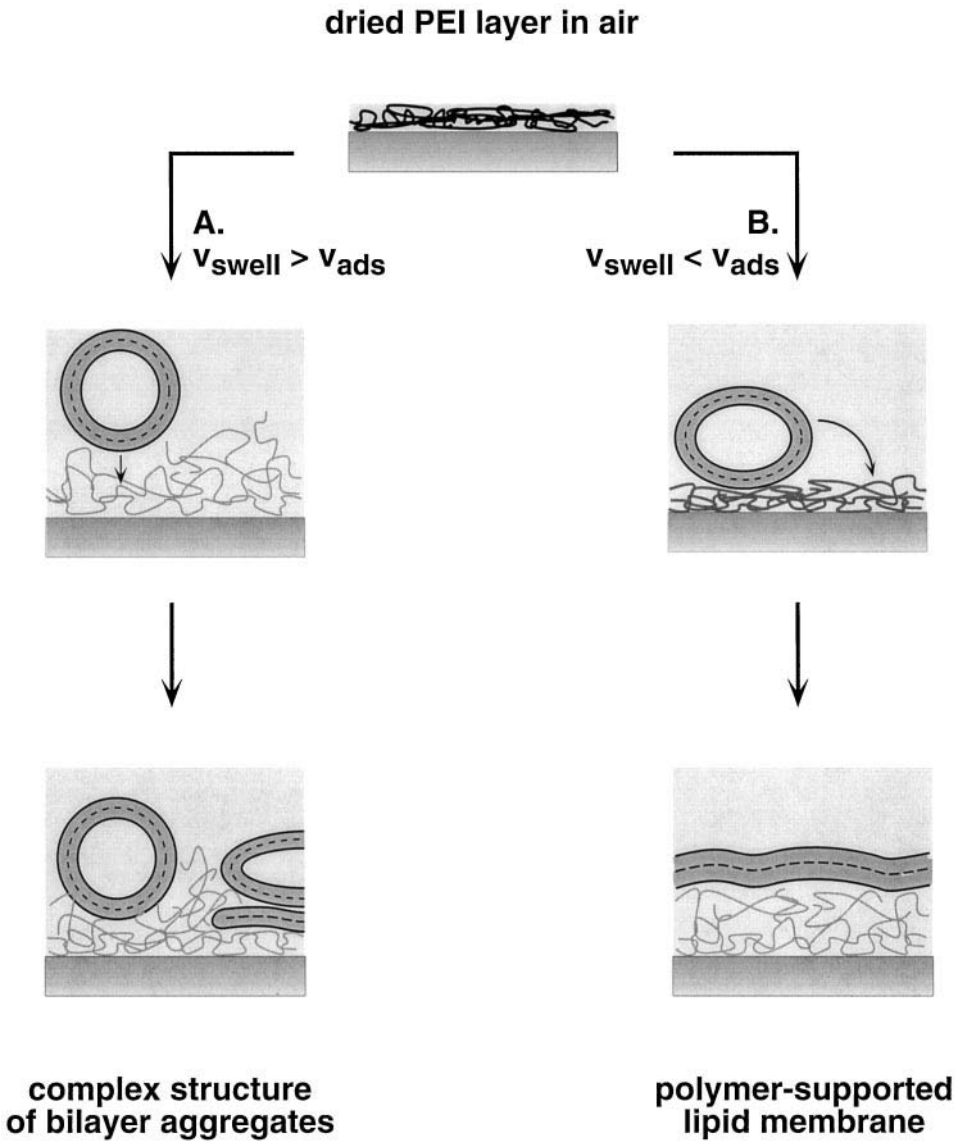

FIGURE 8 A schematic illustration of vesicle adsorption to polymer layers. (*A*) Formation of complex surface aggregates when swelling of the polymer layer proceeds faster than vesicle adsorption (representative of vesicles addition to wet PEI layers). (*B*) Formation of a polymer-supported lipid bilayer when vesicle adsorption proceeds faster than the polymer swelling (representative of vesicles addition of dried PEI layers).

the proximal zwitterionic lipid monolayer from the PEI substrate, as was observed when no vesicles were present. At the same time, a sufficient amount of the lipid membrane must form early in the process to avoid vesicle trapping inside the aqueous polyelectrolyte layer, which we assume to be the main cause of complex surface-aggregate formation on wet polymer surfaces. Therefore, the quick initial vesicle adsorption to the monolayer surface seems to be an essential feature also in our experiments, and presumably proceeds faster than the swelling of the dry PEI layer. Also, the vesicle suspension added to the monolayer-covered substrate (vesicle fusion on monolayer method) most likely carries a considerable amount of organized lipid molecules at its air-liquid interface. This could also aid the formation of the bilayer structure in the very early stages of the adsorption process.

Finally, the considerable amount of water taken up by the polyelectrolyte support in aqueous solution is an important feature of the investigated PEI-supported DMPC membranes. It should be mentioned that the absolute thickness of the polymer layer located underneath the lipid bilayer varies with the method of preparation. However, the observed differences can be rationalized, as the comparatively thin PEI layer (40–50 Å) formed using the "polymer added to bilayer" method (reverse method) under aqueous conditions appears to result from the limited aqueous space between the pre-formed lipid bilayer and the quartz substrate. In contrast, when PEI is free to adsorb to the quartz substrate from solution, thicker polymer layers are observed. After vesicle adsorption to PEI-supported monolayers the polymer thickness increases threefold from 45 Å in air to ~150 Å in water. This is comparable to the final thickness of the water-swollen polymer cushion (~170 Å) that results from vesicle spreading on previously dried PEI layers (vesicle fusion on dry polymer method).

The swelling of the polymer cushion upon exposure to an aqueous solution is also expressed by the observed change in its composition as deduced from its determined scattering length densities. Note, in all cases, the PEI content of the swollen cushion was ~15–20%. The increase of the water content within the PEI layer in buffer solution (as determined for the vesicle fusion on monolayer method) in turn guarantees a soft aqueous compartment between substrate and lipid membrane. This should allow the supported bilayer to exist in a nearly undisturbed, liquid-crystalline state, and thus mostly retain its related natural properties, most importantly its fluidity. While from the neutron scattering data reported here it can only be concluded that the determined bilayer thicknesses on the PEI substrates are in reasonable agreement with values obtained for fluid DMPC membranes from x-ray diffraction studies (L_α-phase, 37°C, $D_{\text{bilayer}} = 35.5$ Å (Janiak et al., 1976)), our earlier fluorescent microscopy studies on the systems investigated here (Seitz et al., 1999) have already demonstrated lipid mobility within the interfacial structure. Additional proof for the fluidity of PEI-supported DMPC bilayers comes from recent direct force measurements employing the surface forces apparatus (Wong et al., 1999; accompanying paper). The structural information obtained by neutron scattering now allows us to conclude that the obtained interfacial fluid aggregate is indeed a single DMPC bilayer resting on an aqueous PEI cushion.

CONCLUSIONS

We have used neutron reflectivity to study the surface structures resulting from various methods for the preparation of polymer-supported lipid membranes on quartz. We found that vesicle adsorption onto a previously dried PEI layer is perhaps the simplest method that gives the desired structure. Another relatively simple method that we previously reported (DMPC bilayer adsorbed onto substrate *prior* to addition of PEI, i.e., reverse method) was successfully applied to conditions of higher salt concentrations. These polymer-supported bilayers appear to have a higher percent coverage when prepared at higher monovalent salt concentrations.

A more elaborate procedure involves the preparation of the initial (proximal) lipid monolayer by LB deposition, which is of importance when the preparation of more complex model membrane systems is desired. The horizontal dipping method commonly used for the preparation of solid supported bilayers proved unsuccessful for the formation of a complete lipid membrane on polymeric supports. However, vesicle adsorption onto preformed polymer-supported monolayers again gives the desired membrane structure.

In general, it was found in all cases where polymer-supported membranes were formed that the underlying polyelectrolyte gives rise to a considerable aqueous compartment that contains only ~15–20 vol % PEI. For semi-dried PEI layers in air this resulted in a considerable swelling (by a factor up to 3) when exposed to an aqueous vesicle solution.

The DMPC-PEI system we have studied is only the first step in an approach to creating model systems for studying with the SFA, AFM, and electrophysiological techniques. However, these conditions more closely mimic actual cell membrane environments compared to biomembranes *directly* supported on bare substrates. In order to provide such biologically relevant architectures, we plan to study membranes of increased complexity, enhancing their long-term stability through partial covalent fixation of chemically reactive lipids to the underlying soft polymeric support.

APPENDIX

Fitting procedure

Our philosophy was to use the simplest physically reasonable model to fit the experimental data (Fig. 9). We illustrate our approach using the vesicle fusion on monolayer method as an example, where the PEI-DMPC monolayer was exposed to a vesicle solution in D_2O in the flow cell. We began with one-box models for the bilayer, adding additional boxes for the PEI polymer. A single Gaussian roughness was used to smear the interfaces, and the resulting reflectivity obtained from the modeling procedure was

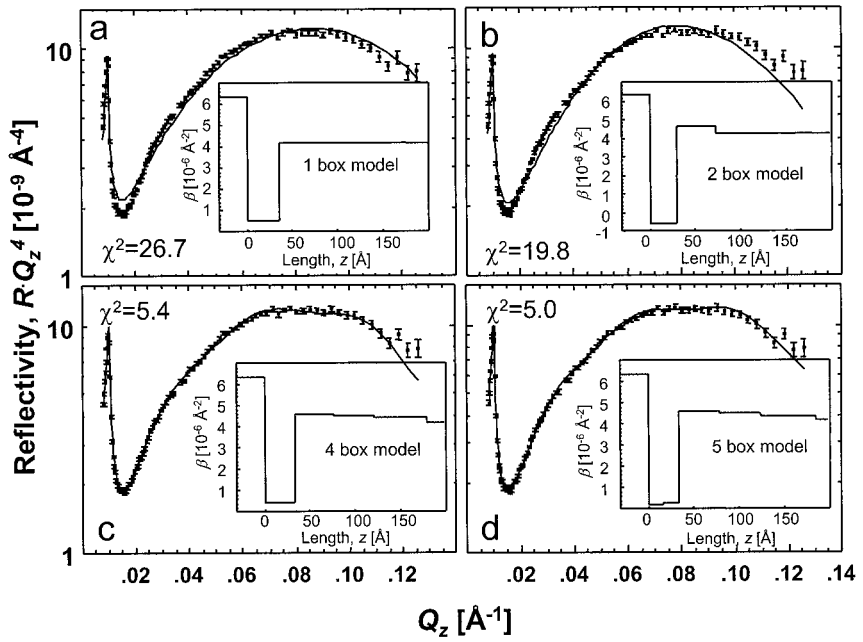

FIGURE 9 (*a–d*) A representative series of fits of increasing complexity for one set of neutron reflectivity data. Each figure contains a scattering length density box model as an inset. The fits were not continued past the point at which χ^2 appeared to reach a plateau. Notice that the fits to the data are best in (*d*); however, we often chose to represent our system with (*c*), since it was a simpler model that does not over-parametrize the problem.

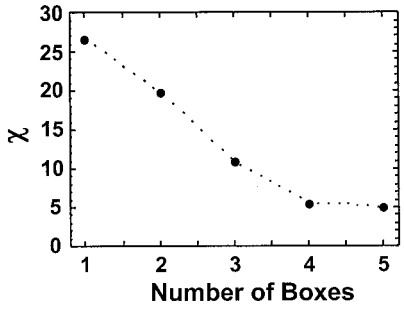

compared to the data. If the simplest model gave a large χ^2 value, we began to increase its complexity by adding boxes to account for the various layers of the interfacial film. The results presented in this work are the best fit to the data using simple, insightful models. Large variations in parameter space were allowed, but we restricted our models to those that generated reasonable results based on the known sizes (length scales) and scattering length densities of the constituent molecules. This enabled us to fit the data with a high level of self-consistency. The three-box model is not shown.

In this paper we present the unsmeared neutron scattering density profiles: profiles without the roughness σ applied. In reality, the neutron scattering length densities are continuous functions of the distance z from the interface. This is shown in Fig. 10, which represents the neutron scattering length density profile shown in Fig. 9 *c, inset* after the Gaussian roughness was applied.

Calculations

We can quantify the amount of water present within the PEI layer by calculating the volume ratio of each component (x and y) and assuming additivity of scattering length densities:

$$\beta_{\text{measured}} = (1 - \phi)\beta_x + \phi\beta_y, \qquad (1)$$

where ϕ is the volume fraction of component y and β is the calculated scattering length density. The scattering length density, β_x or β_y, can be calculated using Eq. 2:

$$\beta_x, \quad \text{or} \quad {}_y = \Sigma b_i/V \qquad (2)$$

where Σb_i is the sum of the scattering lengths of all elements in volume V. For bulk PEI, $\Sigma b_{\text{PEImonomer}} = 0.40 \times 10^{-4}$ Å and assuming $V_{\text{monomer}} \sim 72$ Å^3, we obtain $\beta_{\text{PEI,calc}} = 0.56 \times 10^{-6}$ Å^{-2}. The calculated value of the scattering length densities for D_2O and H_2O is 6.40×10^{-6} Å^{-2} and -0.56×10^{-6} Å^{-2}, respectively.

We can also estimate the surface coverage of the bilayer from the fitted scattering length density of the lipid tails if we assume the second component is mainly D_2O. For the hydrogenated double-chained DMPC tails,

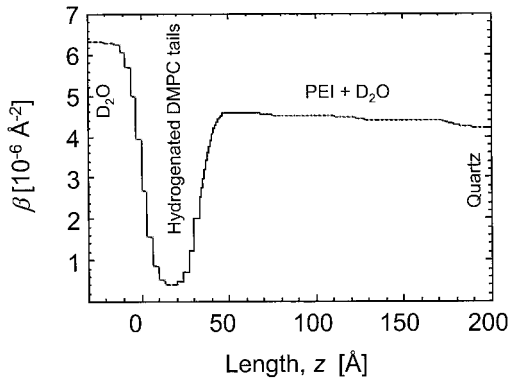

FIGURE 10 The scattering length density profile shown in Fig. 9 *c, inset* smeared by the calculated roughness factor, $\sigma = 6$ Å.

$2\Sigma b_{CH2} = -0.17 \times 10^{-4}$ Å, and if we assume an area per molecule of ~60 Å^2 and a molecular length of 1.26 Å for the CH_2 group, we obtain a value for $\beta_{tails,calc} = -0.22 \times 10^{-6}$ Å^{-2}.

Examples

Determination of the PEI/water composition in the polymer cushion

As an example, the vesicle addition on dried polymer layers method will be discussed. For the dried polyethylenimine layer a fit of the experimental data gave $\beta_{polymer,dry} = -0.30 \times 10^{-6}$ Å^{-2} (Table 1, step (a)). Employing Eq. 1, and using the values for $\beta_{PEI,calc}$ and $\beta_{H2}O$ given above, we calculate $\phi_{PEI,dry} = 0.23$, i.e., the "dry" polymer layer is composed of 23% branched PEI and still carries 77% water (or PEI/H_2O ~ 1:3 v/v). By the same calculation, with $\beta_{PEI,calc}$, β_{D2O} and $\beta_{polymer,wet} = 4.48 \times 10^{-6}$ Å^{-2} (Table 1, step (b)), one finds $\phi_{PEI,wet} = 0.33$ after the addition of the DMPC vesicle suspension in D_2O. This result is highly questionable, since an increase of the PEI content from 23 to 33% to the polymer layer is not only counterintuitive, but also contradicts the observed increase in the layer thickness $D_{polymer}$ from 110 to 180 Å upon addition of D_2O. However, the above calculation based on $\beta_{PEI,calc}$ and β_{D2O} representing the two components of the polymer cushion implicitly requires a complete exchange of H_2O molecules by the added D_2O. Considering the high excess of D_2O added to the system, at first glance, this appears to be a reasonable assumption.

However, it cannot be ruled out that some of the H_2O molecules stay attached to the polyamine, e.g., by hydrogen bonding for which a PEI-H_2O interaction should be favored over PEI-D_2O. It is therefore illustrative to recalculate the value for $\phi_{PEI,wet}$ for another extreme case in which one would assume that all of the H_2O present in the "dry" polymer layer remains associated with the PEI even after addition of the vesicle suspension in D_2O. Hereby, instead of $\beta_{PEI,calc}$, the scattering length density $\beta_{PEI/H2O} = -0.3 \times 10^{-6}$ Å^{-2} is used in the calculation, which was determined for the polymer layer before the addition of D_2O. This results in $\phi_{PEI/H2O,wet} = 0.29$. With $\phi_{PEI,dry} = 0.23$, one obtains $\phi_{PEI,wet} = \phi_{PEI/H2O,wet} \times \phi_{PEI,dry}$, which gives a lower boundary of ~7% for the amount of PEI in the polymer layer.

It is apparent that neither of the two approaches for the calculation of the polymer layer's composition based on the determined scattering length densities $\beta_{polymer}$ gives an entirely reliable result, so that the two calculated values for $\phi_{PEI,wet}$ could be seen as an upper and lower boundary for the PEI content in the water swollen polymeric substrate.

An additional consideration comes from the observed thickness change of the polymer layer, $D_{polymer}$. If no PEI is lost during the vesicle adsorption process, and no other material affects the layer thickness other than the added D_2O, a swelling factor, $f_{swell} = D_{polymer,wet}/D_{polymer,dry} = 1.64$, can be calculated. The swelling factor relates the PEI content in the dried and the swollen polymer cushion by

$$\phi_{PEI,wet} = \phi_{PEI,dry}/f_{swell}, \quad (3)$$

so that $\phi_{PEI,wet} = 0.14$ is easily calculated.

In a similar fashion, when the polymer-supported membrane is prepared by vesicle adsorption onto LB monolayers of DMPC on PEI/quartz, a PEI content of 33% is calculated when assuming a complete H_2O/D_2O exchange in the polymer cushion (before, a composition in the dried state, PEI/H_2O ~ 1:1 (v/v) was determined for the DMPC monolayer in air). For the case where H_2O is assumed to stay associated with the PEI, a concentration of only 14% polymer is calculated. Again, the latter value agrees better with a calculation based on the observed thickness changes. Based on these considerations, a value of 15–20 vol % appears to be a reasonable estimate for the PEI-content in the aqueous compartment supporting the DMPC bilayer membrane.

Determination of the surface coverage with lipid bilayer

A similar calculation gives us an estimate of the quality of the obtained polymer-supported membranes expressed as the surface area covered by the lipid layer. In this case, Eq. 1 together with $\beta_{tails,calc}$ and β_{D2O} can be used to calculate ϕ_{lipid} from $\beta_{lipidtails}$. For DMPC bilayers prepared by vesicle adsorption on dried PEI layers, this gives $\phi_{lipid} = 0.94$, i.e., an almost complete coverage of the polymer substrate with lipid bilayer.

As for the determination of the PEI/water ratio in the polymer cushion, the choice of the β values for the two components forming the layer is important. In the calculation above, it was assumed that holes in the bilayer (or uncovered regions of the substrate) would consist of only D_2O. It could also be argued that the underlying, swollen polymer cushion can stretch out to some extent and partially fill up such bilayer holes. However, this issue seems to be less critical here. If, instead of β_{D2O}, the value $\beta_{polymer}$ of the underlying polymer cushion is chosen as the second contribution to the overall $\beta_{lipidtails}$, one still obtains a similar but slightly lower value, $\phi_{lipid} = 0.93$. This result directly relates to the reasonably highest possible amount of PEI disturbing the bilayer region, and gives a lower boundary for the "integrity" of the lipid membrane on the polymer substrate. As the deviation between the two values for ϕ_{lipid} was generally <5%, only the numbers calculated based on β_{D2O} and $\beta_{tails,calc}$ are given throughout this paper (i.e., neglecting a possible contribution by $\beta_{polymer}$).

This work was supported (in part) under the auspices of the United States Department of Energy. The Manuel Lujan Jr., Neutron Scattering Center is a national user facility funded by the United States Department of Energy, Office of Basic Energy Sciences-Materials Science, under contract number W-7405-ENG-36 with the University of California. The work at UCSB was supported by the MRL Program of the NSF under No. DMR-9123048, and by a National Institutes of Health-NRSA individual postdoctoral fellowship GM17876 (to J.Y.W.). M.S. acknowledges partial funding by the Deutsche Forschungsgemeinschaft (fellowship Se 855/1-1).

REFERENCES

Als-Nielsen, J. 1986. Synchrotron x-ray studies of liquid-vapor interfaces. *Physica.* 140A:376–389.

Baker, S. M., P. D. Butler, W. A. Hamilton, J. B. Hayter, and G. S. Smith. 1994. Shear cell for the study of liquid-solid interfaces by neutron reflectometry. *Rev. Sci. Instrum.* 65:412.

Bangham, A. D., M. W. Hill, and N. G. Miller. 1974. Preparation and use of liposomes as models of biological membranes. *Methods Membr. Biol.* 1:1–68.

Bayerl, T. M., and M. Bloom. 1990. Physical properties of single phospholipid bilayers adsorbed to micro glass beads: a new vesicular model system studied by H-2-nuclear magnetic resonance. *Biophys. J.* 58: 357–362.

Elender, G., and E. Sackmann. 1994. Wetting and dewetting of Si/SiO2-wafers by free and lipid-monolayer covered aqueous solutions under controlled humidity. *Journal de Physique II*. 4:455–479.

Evert, L. L., D. Leckband, and J. N. Israelachvili. 1994. Structure and dynamics of ion-induced domains in free and supported monolayers and bilayers. *Langmuir*. 10:303–315.

Hinterdorfer, P., G. Baber, and L. K. Tamm. 1994. Reconstitution of membrane fusion sites: a total internal reflection fluorescence microscopy study of influenza hemagglutinin-mediated membrane fusion. *J. Biol. Chem.* 269:20360–20368.

Horn, R. G. 1984. Direct measurement of the force between two lipid bilayers and observation of their fusion. *Biochim. Biophys. Acta*. 778: 224–228.

Jacobson, K., E. D. Sheets, and R. Simson. 1995. Revisiting the fluid mosaic model of membranes. *Science*. 268:1441–1442.

Janiak, M. J., D. M. Small, and G. G. Shipley. 1976. Nature of the thermal pretransition of synthetic phospholipids: dimyristoyl and dipalmitoyllecithin. *Biochemistry*. 15:4575–4580.

Johnson, S. J., T. M. Bayerl, D. C. McDermott, G. W. Adam, A. R. Rennie, R. K. Thomas, and E. Sackmann. 1991. Structure of an adsorbed dimyristoylphosphatidylcholine bilayer measured with specular reflection of neutrons. *Biophys. J.* 59:289–294.

Kalb, E., S. Frey, and L. K. Tamm. 1992b. Formation of supported planar bilayers by fusion of vesicles to supported phospholipid monolayers. *Biochim. Biophys. Acta*. 1103:307–316.

Kalb, E., and L. Tamm. 1992a. Incorporation of cytochrome b5 into supported phospholipid bilayers by vesicle fusion to supported monolayers. *Thin Solid Films*. 210/211:763–765.

Koenig, B., S. Krueger, W. J. Orts, C. F. Majkrzak, N. F. Berk, J. V. Silverton, and K. Gawrisch. 1996. Neutron reflectivity and atomic force microscopy studies of a lipid bilayer in water adsorbed to the surface of a silicon single crystal. *Langmuir*. 12:1343–1350.

Kuhl, T. L., J. Majewski, J. Y. Wong, S. Steinberg, D. E. Leckband, J. N. Israelachvili, and G. S. Smith. 1998. A neutron reflectivity study of polymer-modified phospholipid monolayers at the solid-solution interface: polyethylene glycol-lipids on silane-modified substrates. *Biophys. J.* 75:2352–2362.

Kühner, M., and E. Sackmann. 1996. Ultrathin hydrated dextran films grafted on glass: preparation and characterization of structural, viscous, and elastic properties by quantitative microinterferometry. *Langmuir*. 12:4866–4876.

Kühner, M., R. Tampe, and E. Sackmann. 1994. Lipid mono and bilayer supported on polymer films: composite polymer-lipid films on solid substrates. *Biophys. J.* 67:217–226.

Lingler, S., I. Rubinstein, W. Knoll, and A. Offenhausser. 1997. Fusion of small unilamellar lipid vesicles to alkanethiol and thiolipid self-assembled monolayers on gold. *Langmuir*. 13:7085–7091.

Majewski, J., J. Y. Wong, C. K. Park, M. Seitz, J. N. Israelachvili, and G. S. Smith. 1998. Structural studies of polymer-cushioned lipid bilayers. *Biophys. J.* 76:2363–2367.

McConnell, H. M., T. H. Watts, R. M. Weis, and A. A. Brian. 1986. Supported planar membranes in studies of cell-cell recognition in the immune system. *Biochim. Biophys. Acta*. 864:95–106.

Nevot, L., and P. Croce. 1980. Characterisation of surfaces by grazing x-ray reflection. *Rev. Phys. Appl.* 15:761–779.

Paddeu, S., F. Antolini, T. Dubrovsky, and C. Nicolini. 1995. Langmuir-Blodgett film of glutathione s-transferase immobilized on silanized surfaces. *Thin Solid Films*. 268:108–113.

Puu, G., and I. Gustafson. 1997. Planar lipid bilayers on solid supports from liposomes: factors of importance for kinetics and stability. *Biochim. Biophys. Acta*. 1327:149–161.

Russel, T. P. 1990. X-ray and neutron reflectivity for the investigation of polymers. Mater. Sci. Rep. Elsevier (Holland) 5:171–271.

Sackmann, E. 1996. Supported membranes: scientific and practical applications. *Science*. 271:43–48.

Salafsky, J., J. T. Groves, and S. G. Boxer. 1996. Architecture and function of membrane proteins in planar supported bilayers: a study with photosynthetic reaction centers. *Biochemistry*. 35:14773–14781.

Seitz, M., C. K. Park, J. Y. Wong, and J. N. Israelachvili. 1999. Study of the fusion process between solid- and soft-supported phospholipid bilayers with the surface forces apparatus. *In* ACS Symposium Series: Supramolecular Structure in Confined Geometries. G. Warr and S. Manne, editors. ACS, Washington, D.C. In press.

Seitz, M., J. Y. Wong, C. K. Park, N. A. Alcantar, and J. Israelachvili. 1998. Formation of tethered supported bilayers via membrane-inserting reactive lipids. *Thin Solid Films*. 327–329:767–771.

Spinke, J., J. Yang, H. Wolf, M. Liley, H. Ringsdorf, and W. Knoll. 1992. Polymer-supported bilayer on a solid substrate. *Biophys. J.* 63: 1667–1671.

Steinem, C., A. Janshoff, W. P. Ulrich, M. Sieber, and H. J. Galla. 1996. Impedance analysis of supported lipid bilayer membranes: a scrutiny of different preparation techniques. *Biochim. Biophys. Acta-Biomembr.* 1279:169–180.

Tamm, L. K., and H. M. McConnell. 1986. Supported phospholipid bilayers. *Biophys. J.* 47:105–113.

Wong, J. Y., C. K. Park, M. Seitz, and J. Israelachvili. 1999. Polymer-cushioned bilayers II. An investigation of interaction forces and fusion using the surface forces apparatus. *Biophys. J.* 77:1458-1468.